CHALMERS
UNIVERSITY OF TECHNOLOGY

Potential tellurium deposits in the BWR containment during a severe nuclear accident

Downloaded from: https://research.chalmers.se, 2024-04-26 07:40 UTC

Citation for the original published paper (version of record):
Espegren, F., Ekberg, C. (2020). Potential tellurium deposits in the BWR containment during a severe nuclear accident. Annals of Nuclear Energy, 146. http://dx.doi.org/10.1016/j.anucene.2020.107629

N.B. When citing this work, cite the original published paper.

research.chalmers.se offers the possibility of retrieving research publications produced at Chalmers University of Technology.
It covers all kind of research output: articles, dissertations, conference papers, reports etc. since 2004.
research.chalmers.se is administrated and maintained by Chalmers Library

(article starts on next page)

Annals of Nuclear Energy 146 (2020) 107629

Contents lists available at ScienceDirect

Annals of Nuclear Energy

journal homepage: www.elsevier.com/locate/anucene

Potential tellurium deposits in the BWR containment during a severe nuclear accident

Fredrik Espegren *, Christian Ekberg

Department of Chemistry and Chemical Engineering, Nuclear Chemistry and Industrial Materials Recycling, Chalmers University of Technology, kemivägen 4, SE-412 96 Göteborg, Sweden

ARTICLE INFO

Article history:
Received 7 February 2020
Received in revised form 19 May 2020
Accepted 1 June 2020
Available online 16 June 2020

Keywords:
Fission products
Tellurium
Te transport
Nuclear accidents
BWR
Containment
Deposits

ABSTRACT

The release of fission products to the environment is one of the concerns with nuclear power. During an accident, the most likely released are the volatile fission products i.e., tellurium. To evaluate the behavior of tellurium in the event of an accident, it was heated under different conditions (oxidizing, inert, reducing; both dry and humidified). The formed vapor was transported to surfaces (aluminum, copper, zinc) at room temperature that can be found in the BWR-containment.

All formed deposits were examined for morphology and species. Moreover, the content of sodium hydroxide liquid traps following the metal surfaces and filter was also investigated. In these traps, the highest amount of tellurium was found under humid-reducing followed by humid-oxidizing conditions. In the deposit removed from the zinc surface acquired under the latter conditions, elemental analysis observed zinc, indicating a possible reaction between tellurium and zinc. The corresponding trap showed significant amounts of zinc.

© 2020 The Author(s). Published by Elsevier Ltd. This is an open access article under the CC BY license (http://creativecommons.org/licenses/by/4.0/).

1. Introduction

In the event of a nuclear accident, the release of fission products (FP:s) is considered one of the main issues. Thus, investigation of the behavior regarding these elements will help in understanding both the mechanisms of release and in the end potential for mitigation. Factors to be understood for the important FP:s includes the type, magnitude, consequences, and potential risks with such releases (can be referred to as source term) (Ducros, 2012).

Historically, the FP iodine has been the main focus of the research community. This is due to the very high volatility of several iodine species (Ducros, 2012), complexation with organics (Bosland et al., 2014), and accumulation in the human thyroids (Yoshida et al., 2014). The latter makes it possible for a substantial dose to the population. However, another FP that is of concern is tellurium. The two main reasons for this are the high volatility of tellurium and its highly reactive nature (Alonso and González, 1991). Moreover, as some of the tellurium isotopes (e.g., ^{131}Te, ^{132}Te, ^{133m}Te, ^{134}Te representing 60 % of the activity of tellurium in the fuel Alonso and González, 1991) decays to iodine (Magill et al., 2015), any releases of tellurium will subsequently result in increases of the iodine source term. Observing the core content at shut down for a Peach Bottom boiling water reactor (BWR), these two FPs estimated amounts are 9.63 EBq and 30.5 EBq of tellurium and iodine respectively (Bixler et al., 8718). Consequently, the tellurium source term needs to be well understood to fully evaluate the source term of iodine.

When it comes to tellurium speciation and behavior inside the containment, knowledge is scarce. This fact has been indicated early on by Collins et al. (1987) as well as Beahm (1987) and later on by McFarlane (1996). However, knowledge prior to entering the containment exists and an important factor for tellurium releases and characteristics at these stages, consequently to the containment, is the prevailing conditions. Before a reactor core melt occurs or prior to temperatures becoming too high (around 2350 °C Pontillon et al., 2010), the cladding needs to be fully oxidized for there to be substantial releases of tellurium (de Boer and Cordfunke, 1997; de Boer and Cordfunke, 1995). Depending on the oxygen potential of the prevailing condition, the chemical speciation of the tellurium releases can vary from SnTe (de Boer and Cordfunke, 1997), Te/Te_2 (Alonso and González, 1991), TeO (Alonso and González, 1991) (high temperatures required), TeO_2 (Alonso and González, 1991), $TeO(OH)_2$ (Alonso and González, 1991; Malinauskas et al., 1970; Dutton and Cooper, 1966) (transient and requires water to form), Cs_2Te (McFarlane, 1996; Imoto and Tanabei, 1988) (dissociates at high temperature), to H_2Te (Alonso and González, 1991) (formed at high temperature under

* Corresponding author.
E-mail address: espegren@chalmers.se (F. Espegren).

https://doi.org/10.1016/j.anucene.2020.107629
0306-4549/© 2020 The Author(s). Published by Elsevier Ltd.
This is an open access article under the CC BY license (http://creativecommons.org/licenses/by/4.0/).

reducing and humid reducing conditions). Of these, this work will focus on Te (main species under inert/reducing conditions) and subject it to different experimental conditions to alter it to relevant mix of species (under dry and humid reducing; e.g., H_2Te and dry and humid oxidizing; e.g,. TeO, TeO_2, $TeO(OH)_2$). The melting and boiling points of some the these compounds can be found in Table 1.

Several different types of surfaces can be found in the containment of a nuclear power plant. This work will be limited to the study of aluminum, copper, and zinc at close to room temperature. The surface choices (Glänneskog et al., 2006; Holm et al., 2009; Kajan et al., 2016) are based on the Swedish BWR, where it has been estimated that these metals have a surface area of: 11 930 m^2 construction material of aluminum, 6 300 m^2 of galvanized metal (i.e. zinc), and 1 350 m^2 of copper aerosol covered surfaces (i.e., produced during the accident) (Kajan et al., 2016). The latter originates from the copper cables producing aerosols (average diameter of 10 μm) (Kajan, 2016; Glänneskog, 2005). Furthermore, more zinc may be present in the paint covering stainless steel surfaces (Tietze, 2015). Some compound between tellurium and these compounds can be observed in Table 1. Observing existing literature, it is expected that temperatures in the containment will be below 140 °C (Mun et al., 2006). Thus, this work (similar to previous work Glänneskog et al., 2006) aims to be below that values. Limiting these experiments to room temperature was to determine what would remain at the lower end of the temperature range.

The aim of this paper is to address the previously mentioned lack of knowledge through experiments designed to simulate the behavior of tellurium as it enters the containment from the reactor coolant system and to determine how the deposition occurs on surfaces found therein (aluminum, copper, and zinc) and concurrently acquire knowledge of tellurium transport. Three different conditions (oxidizing, inert, and reducing) were investigated, both without and with humidity. These experiments were carried out using a furnace to heat the tellurium, which volatilized and transported the tellurium to the metal surfaces.

2. Experimental

All experimental work were performed using a tube furnace (ETF 30-50-18-8, Entech), in which a 130 cm long high purity alumina tube (Al_2O_3, 99.7%, Degussit AL23, Aliaxis) was placed. Connectors (stainless steel, custom-made) were attached at each end. The inlet was fitted with two gas inlets, to simplify the change of gas. Moreover, to enable humid conditions an atomizer (Constant Output Atomizer, Model 3076, TSI Incorporated) was connected for the relevant experiments prior to the inlet connection and was filled with water (500 ml, Millipore 18 MΩ). The outlet connector was designed with an interior of a cone to promote a smoother transition for the exiting gas flow. Moreover, this design also allowed a filter (Merck™ Mitex™ PTFE Membrane Filters, pore size 5 μm, thickness 125 μm cut to fit) to be located at the exit. Two gas traps were connected in a row to the outlet. The first contained sodium hydroxide (pellet, ⩾97%, Sigma Aldrich) solution (0.1 M, 250 ml) to trap gaseous species and the second trap was filled (250 ml) with water (water, Millipore 18 MΩ) to reduce the amount of potential gas escaping. A schematic overview can be seen in Fig. 1.

The tellurium (99.8%, 200 mesh, Sigma Aldrich) precursor was used without any pretreatment. The precursor amount (1 g) was the same for all experimental conditions and was evenly spread out in a crucible. Two types of crucibles were used, one type for the oxidizing and inert conditions (boat, porcelain 85 × 13 × 8 mm, VWR), and another for the reducing condition (Al_2O_3-material). The reason for this was that under reducing condition, the first type became heavily corroded under trial-testing and was therefore determined not to be suitable for use under reducing condition. No, significant damage was observed for the first type of crucible under the other two conditions.

Table 1
Some different tellurium compounds and some corresponding relevant characteristics (Rumble, 2019).

Compund/Element	Color	MP*	BP**
Te	Gray-white	449.51	988
TeO_2	White	733	1245
TeO_3	Yellow-orange	430	
H_2Te		−49	−2
H_2TeO_3	White	40, dis.***	
H_6TeO_6	White	136	
Al_2Te_3	Gray-black	≈ 895	
CuTe	Yellow	trans.**** ≈ 400	
Cu_2Te	Blue	1127	
$CuTeO_3$	Black, glassy		
Al_2Te_3	Grey-black	≈ 895	
ZnTe	Red	1295	

*melting point; **boiling point; ***dissociation; ****transition.

The surfaces that were investigated, had to be cut into suitable sizes, either from a rod or a sheet. An aluminum rod (ø: 19 mm, 99.5% Alfa Aesar) and a zinc rod (ø: 13 mm, 99.5% Alfa Aesar) were cut into 3 mm thick discs. The copper, was cut into 10x10 mm squares from a sheet (thickness: 3 mm, 99.5% Alfa Aesar). Prior to the experiments, all coupon surfaces were cleaned with acetone, ethanol, and water (Millipore 18 MΩ) in the order stated. These surfaces were located in a row in the following order: copper, zinc, and aluminum on a crucible at the outlet of the tube (surrounding gas flow was close to room temperature[1]).

The crucibles containing the precursor used during the experiments were positioned inside the tube so that they were always located in the middle of the furnace. At this location, the isothermal temperature (1000 °C) was maintained for a set amount of time (1 h), after being heated (10 °C/min) from ambient temperature.

During heating, the flow of an inert gas (nitrogen, in–house gas[2]) was maintained during the initial heating phase (until 400 °C) to establish pre-accident conditions. After this phase the flow was halted until isothermal temperature was reached. This procedure ensured no volatilized precursor material was transported away prior to reaching the isothermal temperature. Once isothermal temperature was reached, the initiation of the gas flow was delayed (10 min) to ensure that the isothermal temperature was stable. Following this the desired gas flow was initiated (1–2 l/min[3]) and maintained (50 min).

To establish the different experimental conditions, and to concurrently act as a carrier gas for the transportation of the volatilized species, three types of gases were used. These three gases corresponded to oxidizing (compressed air, Porter gas regulator), inert (Ar, 99.999%, Air liquid, Aalborg gas regulator), and reducing (Ar with $5\%_{mol}$ H_2, Air liquid, Aalborg gas regulator) conditions. When humid conditions were investigated, the atomizer was used and filled with water. Hence, the total amount of experiments performed becomes six (no replicates). An experimental matrix can be found in Table 2.

Additionally, reference cases were carried out to determine the different experimental conditions effect on the surfaces. These references were performed as the actual experiment in an unused tube, but without the tellurium present.

[1] Verified with a N-thermocouple, during pre-trials.
[2] According to responsible personal, 99.9% purity. However, not certified nor verified.
[3] Slightly lower during humid conditions, due to limitation of the atomizer.

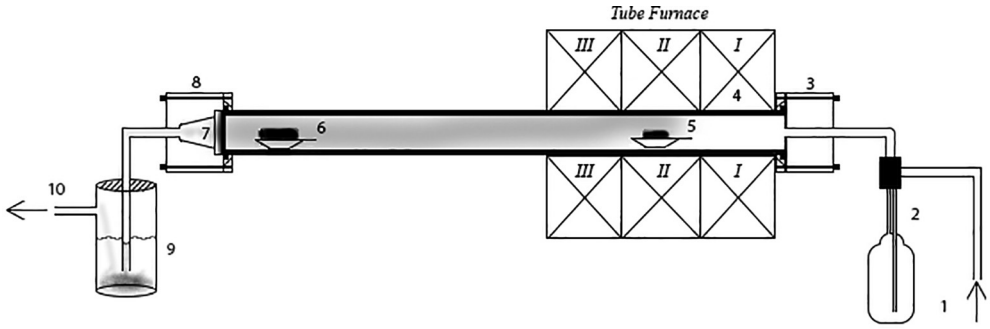

Fig. 1. The experimental schematics: (1) gas inlet, (2) atomizer, (3) inlet, (4) Al_2O_3-tube, (5) the precursor location, (6) the metallic coupon, (7) filter, (8) connector, (9) a sodium hydroxide solution (0.1 M) trap, and a water trap, and (10) the gas outlet.

Table 2
An overview of the experiments. Relative humidity (RH) determined at the outlet with the furnace heated to 1000 °C) and a temperature of 27 °C at the measuring location, using a Fisherbrand™ Traceable™ humidity meter.

Experiment	Atmosphere	Main gas	RH [%]	Surfaces
1	Oxidizing	Compressed air	0.1	Cu, Zn, Al
2	Oxidizing	Compressed air	97	Cu, Zn, Al
3	Inert	Argon	0.1	Cu, Zn, Al
4	Inert	Argon	99	Cu, Zn, Al
5	Reducing	Argon/5%hydrogen	0.1	Cu, Zn, Al
6	Reducing	Argon/5%hydrogen	99	Cu, Zn, Al

3. Results and discussion

The outcome of the experiments performed in this study was evaluated both quantitatively and qualitatively. Methods included standard laboratory balance (mass of deposits on filters), inductively coupled plasma mass spectrometry (ICP-MS, content of the sodium hydroxide liquid traps), scanning electron microscopy (SEM, morphology of the particles found in the deposit on the metal surfaces) coupled with energy dispersive X-ray spectroscopy (EDX, elemental composition of the particles found in the deposit on the metal surfaces), and glancing angle X-ray diffraction spectroscopy (XRD, speciation of the deposits on the filters and the metal surfaces).

3.1. Quantitatively

As no online monitoring of the volatilized precursor was possible, three reference points for tellurium releases were chosen: (1) weight of what was left in the crucible, (2) mass increase of the filter due to deposition, and (3) content of the sodium hydroxide liquid trap. This to gain some knowledge regarding the transport behavior of tellurium under the investigated conditions.

Considering that the measurements made on the standard laboratory balance (Ohaus Explorer®) is not highly accurate, only two decimals are included. However, small weights of known mass were used to verify (VWR ZWIEBEL,1 g and 100 mg) that the weight shown by the balance was not too far off.

An ICP-MS (Thermo Scientific™ iCap Q ICP-MS) was used to determine the amount of tellurium and the three metals in the sodium hydroxide liquid traps. The samples were diluted from 0.5 ml of the original solution using nitric acid (0.5 M, ultra-pure HNO_3, Sigma Aldrich) with an internal standard (10 μg/l of rhodium, element standard foratomic spectroscopy 1000 ± 5 mg/ml, 20 °C, Spectrascan). The evaluation of the data was performed using Qtegra™ Intelligent Scientific data solution (v.2.21465.44).

3.2. Qualitatively

SEM (Quanta 200 FEG ESEM) coupled with EDX was used to indicate the elemental composition and the morphology of the particles in the deposit formed on the metal surfaces. To enable the analyses, a part of the deposit was removed from each surface of the metal coupons using the adhesive side of a carbon tape. Hence, sized determination of the particles would not be accurate from these micrographs and only a general description is provided of the observed sizes. All micrographs were obtained using the same configuration and distance (15 kV, at a magnification of ×3600 relative to the surface of the object). Furthermore, several objects/locations were investigated by EDX. However, only three or four of these are presented in the results section for the SEM/EDX analysis and the individual spectrum of each location can be found in Appendix A. The elemental composition gained from the EDX was used as a foundation for the XRD analyses.

XRD (Siemens Diffraktometer D5000, CuK-α characteristic radiation wavelength) analysis was used with the glancing angle approach as described by B.A. van Brussel and J.Th.M. De Hosson (van Brussel and De Hosson, 1994). All the deposits on the metal surfaces were investigated with this approach[4]. For each deposit, the angle had to be adjusted accordingly (due to manual leveling of the surface level in relation to the X-ray beam). Therefore, the angled used is different for all deposits and is not known relative to the surface of the object. However, two angles (5° and 1°, based on trial and error) were chosen relative to the sample placeholder of which the ones resulting in the clearest diffraction peaks were included in this work. For the deposits on the filters, analyses were performed with the detector and X-ray generator coupled. As the filter itself was not expected to produce any noticeable signal. The observed diffraction peaks were matched using the software (DIFFRAC.SUITE EVA, Bruker AXS version 4.1.1) and according to the database (The International Centre for Diffraction Data, PDF-4 + 2019 RDB) used in conjunction with the XRD equipment. For all diffractograms, the elements were limited to tellurium, oxygen, and aluminum, copper, or zinc (the latter three, depending on the underlying surface). During all analyses, the sample holder was rotating (360°/min) with the detector measuring angle moving from 10° to 90°.

[4] Increasing the diffraction peaks corresponding to the deposit in relation to the bulk material.

For the XRD-diffractograms, the results were post-processed. This was done by reducing the intensity of the whole spectrum (only done on an as needed basis) and each diffractogram was processed according to the "Baseline Estimation and Denoising With Sparsit"-method, described by Ning et al. (2014). None of the results were altered to the point that any distinct diffraction peaks disappeared.

3.3. General observations

It has been observed in this work that the deposition of tellurium in the containment, once exposed to different conditions at high temperature, produces deposits on all types of investigated surfaces under all conditions at room temperature.

Initial visual observation revealed little indications that the underlying surface had any significant effect on the formation or characteristics of the deposit. Thus, there was almost no difference between the depositions formed on the different surfaces within each experiment observable by the naked eye. However, from these no definite conclusions can be made. Possibly, through the analytical analysis, an effect was observed in the case regarding zinc under humid oxidizing conditions, and for aluminum under humid inert and humid reducing conditions. Furthermore, measurable levels of tellurium reached the sodium hydroxide liquid traps during the humid reducing, humid oxidizing, and dry oxidizing conditions.

After each experiment, the filters, crucibles, and metal coupons were weighed to determine the mass changes that had occurred. However, although deposits were observable on the metal coupons and the residue was left in the crucibles used, these did not result in any noticeable mass change measured by the balance. Therefore, they were omitted and the remaining weights are reported in Table 3.

The values in Table 3 show that a mass increase occurred for all filters, roughly doubling the weight of the filters. Observing the weight of the crucibles, little mass change can be seen. Nevertheless, all the crucible had minor residues left in them.

Table 3
The mass of the filters used during each experiment. Weights are shown before and after the experiments.

Conditions	Filter	
	m_{Before} [mg]	m_{After} [mg]
Oxidizing	0.15	0.26
Oxidizing, humid	0.15	0.29
Inert	0.15	0.33
Inert, humid	0.15	0.3
Reducing	0.16	0.3
Reducing, humid	0.16	0.32

3.4. Oxidizing conditions

For the dry and humid oxidizing conditions, the general appearance of the samples when removed from the setup was that a thin white layer had formed on all the metal surfaces (the different metal surfaces were seen through the deposits). Based on the color alone, most likely species would be TeO_2 (Rumble, 2019). For the SEM/EDX analyses, a minor part of each deposit was removed with the adhesive side of a carbon tape. Observation by the naked eye while doing this indicated that the underlying surfaces were seemingly unaffected by the deposits. However, it is not clear from this observation alone if nothing had occurred. Hence, further investigation was needed. The filters located at the end of the tube under both conditions had a similar white deposit (likely TeO_2 Rumble, 2019) and also some part that was slightly blacker (likely Te Rumble, 2019). Moreover, the crucibles used during these experiments were found to have a yellow glaze on the surfaces where the precursor had been added prior to the experiments.

The general morphology of the particles in all the deposits from the two oxidizing conditions on the different surfaces contained smooth round spheres, with varying size distribution. No significant difference was observed between the dry and humid oxidizing conditions. The micrographs of these deposits from the aluminum, copper, and zinc coupons can be seen in Fig. 2. The elemental compositions of the indicated particles can be found in Table 4 and as seen, tellurium, zinc, carbon, and oxygen were the main detected elements. However, the carbon is most likely from the underlying carbon tape. The energy spectra of the locations can be found in Appendix A.

This outcome provides little in the way of conclusive chemical speciation, but instead provides the foundation of the XRD analyses. However, in the case of humid oxidizing conditions zinc was observed in the deposit. One explanation for this could be that something did occur between tellurium and zinc that was enabled by the humid conditions. Alternatively, it could be that the humid oxidizing condition alone removed the zinc. If the former is true a possible explanation could be a reaction with the formed compound $TeO(OH)_2$ (Alonso and González, 1991; Malinauskas et al., 1970; Dutton and Cooper, 1966). This compound forms when water vapor is present together with tellurium dioxide at high temperatures (Malinauskas et al., 1970). However, no literature has been found indicating that this species would react. Furthermore, under the humid conditions a thin water film would form on surfaces, including the zinc surface. This could also be important and necessary for a reaction to take place at all.

Determination of the chemical speciation by XRD analyses indicated that the deposits produced on the different coupons consisted of TeO_2-orthorhombic. When the humidity was increased for the oxidizing conditions, another crystal structure consisting of TeO_2-paratellurite (vertical lines) was observed in the diffractograms. The other non-bulk material diffraction peaks were matched to TeO_2-orthorhombic (dashed vertical lines). These diffractograms (**I** and **II**) can be seen in Fig. 3.

Regarding the deposits from the surfaces of the metals, no major differences were observed in-between the deposits from the different metals under either dry or humid oxidizing conditions. However, comparing the results between the two experimental conditions a noticeable difference can be observed. The difference is the emergence of a new crystalline phase of tellurium dioxide under the humid condition, namely TeO_2-paratellurite. Under dry conditions, the only crystalline phase observed was that of the TeO_2-orthorhombic. Thus, this difference again indicates that something occurred during the humid condition experiment. The previously suggested $TeO(OH)_2$ species (Alonso and González, 1991; Malinauskas et al., 1970; Dutton and Cooper, 1966) occurrence could be the cause of the new crystal structure. Should this be the case, this species would then have to dissociate at lower temperature consequently forming the alternative tellurium dioxide. Alternatively, the new species itself could be trapped on the surfaces, after which it dissociates. Furthermore, if this species reaches the zinc surface it could also be the reason for the detection of zinc by the EDX in the deposits. However, neither the XRD nor the EDX gave clear evidence for this.

The filters used under the two oxidizing conditions were also analyzed using XRD. The corresponding diffractograms can be seen in the image (**III**) in Fig. 3 and show several diffraction peaks, that were identified as TeO_2-paratellurite (all non-indicated maximums) and TeO_2-orthorhombic (vertical dashed lines).

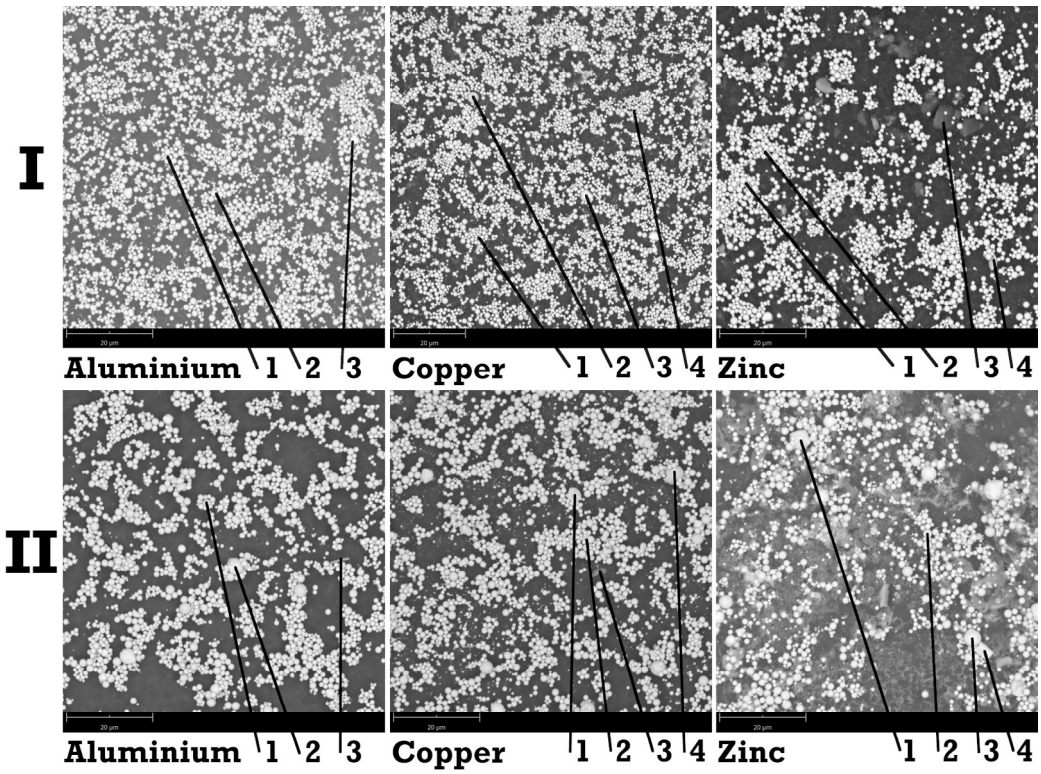

Fig. 2. Six micrographs from dry (**I**) and humid (**II**) oxidizing conditions experiments, each showing the deposits from the aluminum (left), copper (middle), and zinc (right) surfaces. The locations highlighted have been analyzed and the detected elements are shown in Table 4.

Table 4
The main elements detected using energy dispersive X-ray analysis (EDX) on selected points in the micrographs of both oxidizing conditions, shown in Fig. 2. Except for C, all elements detect are included. Appendix A contains the corresponding EDX spectrum.

	Oxidizing				Oxidizing, humid			
Position	1	2	3	4	1	2	3	4
Aluminum	Te, O	Te, O	Te, O	Te, O	Te, O	Te, O	Te, O	
Copper	Te, O	Te, O	Te, O	Te, O	Te, O	Te, O	Te, O	Te, O
Zinc	Te, O	Te, O	Te, O	Te, O	Te, O	Te, O, Zn	Te, O	Te, O

The sodium hydroxide traps from these experiments were analyzed to determine the tellurium and the different metals content. For the dry and humid oxidizing conditions, detectable levels of tellurium were observed in both traps used under the two conditions. Of these two, the humid oxidizing condition contained the most tellurium with a $0.65\%_{weight}$ compared to $0.008\%_{weight}$ for the dry oxidizing condition (percent of the original precursor amounts). Furthermore, in the case of humid oxidizing conditions zinc was also detected in the trap and was determined to be roughly 0.3 mg.

In the depositions formed on the filter under these conditions, both types of crystalline phases of the tellurium dioxide were observed. This indicates that the source of TeO_2-paratellurite might not come from the interaction with water vapor. A possible alternative answer could be the formation of TeO at high temperatures (Alonso and González, 1991). TeO is only stable at high temperatures and thus at a lower temperature it could form the alternative TeO_2-paratellurite. However, this by itself does not explain the difference in the crystal structure observed in the deposits from the surfaces of the two different conditions. Instead, this could be explained by the possible formation of a thin water film on the surfaces that readily absorbs more in total of the tellurium from the gas phase. More of the alternative tellurium dioxide could then appear in the deposit and reach above the XRD lower detection limit. However, regarding the latter it is not possible to clarify this as all the masses of the deposits from both experimental conditions are very small. Moreover, no tellurium zinc compounds were detected in either filter.

Observing the content of the sodium hydroxide liquid traps, it is clear that the addition of humidity increased the amount of tellurium transported. This has already been indicated to occur according to existing literature (Malinauskas et al., 1970) through the formation of $TeO(OH)_2$. Consequently, this species might have had an effect on the size distribution of the transported tellurium, thereby shifting the distribution towards smaller sized particles, be it vapor or small aerosols. The change in size would then allow more tellurium to pass through the filter and thus reach the trap. However, under the same condition a noticeable level of zinc was observed. In the two reference experiments, no noticeable amounts of any of the metals were detected in the traps.

The remaining question is then how the zinc-related observation occurred. A possibility is that a water filmed formed, which could enable the tellurium dioxide to be dissolved and react with the surface. Alternatively a reaction may have occurred between the alternative species ($TeO(OH)_2$ Alonso and González, 1991) formed under humid oxidizing conditions and the surface. This would then have resulted in very minor tellurium zinc complexion forming or possible just enabling releases of zinc. Moreover, if

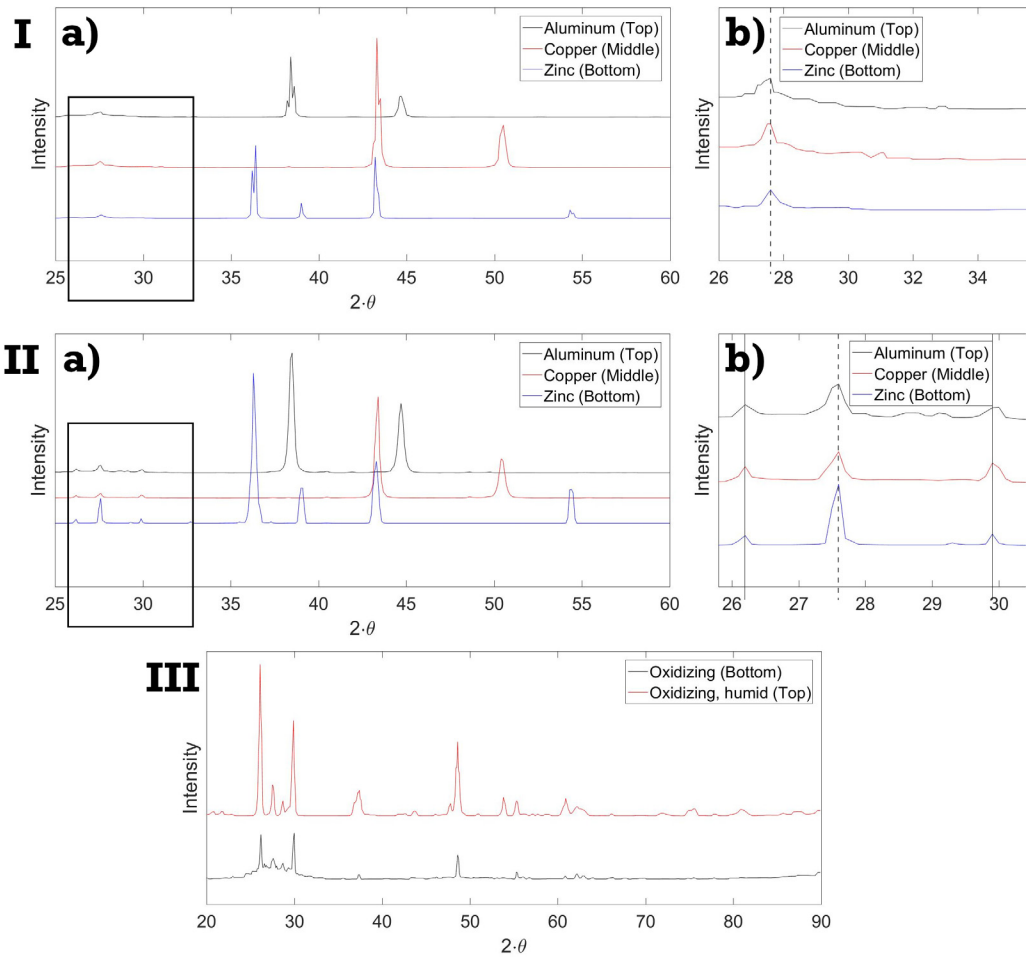

Fig. 3. The X-ray diffraction analyses of the depositions formed on the metal surfaces from dry (**I**) and humid (**II**) oxidizing conditions experiments. Areas highlighted (**I.a** and **II.a**) by boxes are shown to the right (**I.b** and **II.b**). Diffractograms for the filter used during these experiments are also shown (**III**).

something did occur with the surface the effect was minimal to the zinc surface as nothing could be observed with the naked eye. However, no positive speciation with the zinc was possible to clarify this as very little zinc was observed in the deposit. Still, the relative (i.e., if the source was the zinc coupon) high amount of zinc in the trap indicates that something did occur, and this could be the formation of a volatile species (based on it having to pass through the filter and then reaching the trap). Moreover, the reference experiment under the same conditions showed no significant amounts of zinc.

3.5. Inert conditions

Under both dry and humid inert conditions the deposits formed on the different metal surfaces were black and thin (metal surfaces were visible through the deposits formed on top). The black coloration would indicate that it is metallic tellurium (Rumble, 2019). Similarly, as for the samples from the oxidizing conditions experiments, a part of the different surface deposits were removed and showed no change visible to the eye on the metal surfaces. However, it is not clear from this observation alone if nothing had occurred. Moreover, the deposits on the filters showed the same black color with a slightly white/grey coloration. This indicates, based on color (Rumble, 2019) alone metallic tellurium, with possibly some TeO_2 present. Observing the crucibles after these experiments showed a black coloration to the surfaces where the precursor had been added.

Using SEM, the morphology of the particles found in the deposits produced under inert conditions both without and with humidity on the aluminum, copper, and zinc metal surfaces were investigated. The particles found in all these micrographs showed similarly shaped particles, which are a mixture of smooth spheres, clusters of smaller round particles, spike-shaped, and rectangular objects. These micrographs can be seen in Fig. 4. To determine the elemental composition of the locations highlighted in these, EDX analyses were performed at several locations. The EDX analyses showed that tellurium and carbon were found in all locations. Moreover, some locations also contained oxygen. The carbon found, most likely comes from the carbon tape. In Table 5 the outcome of the EDX analysis is shown.

The deposits acquired under dry (**I**) and humid (**II**) inert conditions were analyzed by XRD and diffractograms with diffraction peaks were attained. For both types of inert conditions, the diffraction peaks were matched to metallic tellurium, in addition to the diffraction peaks from the underlying bulk materials. These diffractograms can be seen in Fig. 5. In these images only the diffraction peaks corresponding to metallic tellurium have been highlighted.

Additionally, the XRD diffractograms of the deposits found on the filters from both inert conditions were also acquired. In these two diffractograms, diffraction peaks corresponding to Te were observed and highlighted. No other elements or compounds were detected. The diffractograms produced from the filters (**III**) can be seen in Fig. 5.

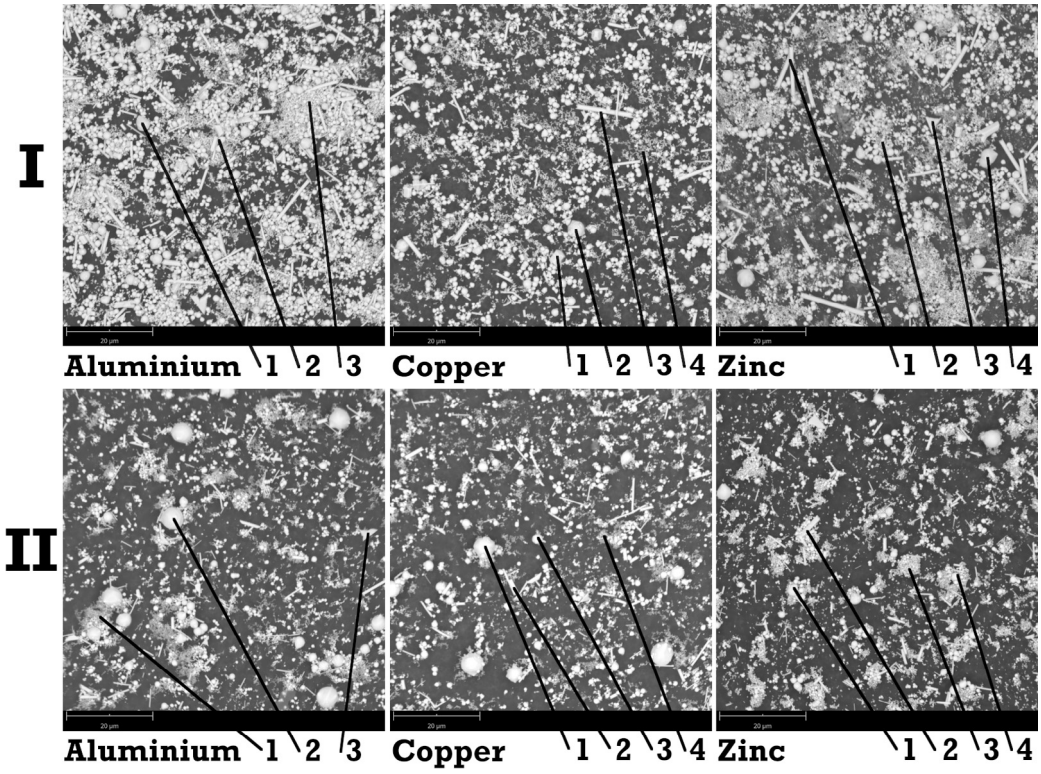

Fig. 4. Six micrographs from dry (**I**) and humid (**II**) inert conditions experiments, each showing the deposits from the aluminum (left), copper (middle), and zinc (right) surfaces. The locations highlighted have been analyzed and the detected elements are shown in Table 5.

Table 5
The main elements detected using energy dispersive X-ray analysis (EDX) on selected points in the micrographs from both inert conditions, shown in Fig. 4. Except for C, all elements detected are included. Appendix A contains the corresponding EDX spectrum.

	Inert				Inert, humid			
Position	1	2	3	4	1	2	3	4
Aluminum	Te	Te	Te		Te, O	Te	Te	
Copper	Te	Te	Te	Te	Te	Te	Te	Te, O
Zinc	Te	Te	Te, O	Te, O	Te	Te	Te	Te

When it comes to the deposits from the surfaces in the inert dry and humid cases, no differences between any of these were observed, neither with regards to morphology nor speciation of the particles. Essentially, the same shaped particles consisting of metallic tellurium were found in all deposits from all types of surfaces. Moreover, this indicates that the underlying surface, regardless of if it is dry or humid, has little effect on the tellurium speciation on the deposits from the metal surfaces under inert condition. This also remained true for the depositions formed on the filters in these experimental conditions, as only metallic tellurium was observed in these deposits. Observing the existing literature (Alonso and González, 1991), this is not unexpected as little change to the gas phase tellurium is expected at low temperature under these conditions. Moreover, some oxygen was observed in some of the locations analyzed by EDX, however, it is not possible from these analyses to clearly state that this is due to the experiments itself or if a small leak occurred during the experiment. Furthermore, it is also possible that there could have been air or other contamination of the sample during transport to the SEM/EDX.

The sodium hydroxide liquid traps from these experiments were analyzed to determine the amount of tellurium and the content of the different metals. However, these analyses showed no significant levels of tellurium in the traps. Only the metal aluminum was noticed in the trap from the humid inert experiments, with a mass of 0.2 mg in the original trap solution.

The aluminum found in the sodium hydroxide liquid trap could be due to the tube being made from aluminum trioxide and therefore minute amounts from the tube walls could have reached the trap. However, it should be noted that the amount is very small and might not be correlated to the experiment. Moreover, observing the weights of the filters used, no significant increase of the masses were observed. This, indicates that the overall tellurium volatility in these cases was low, or was at least prevented, possibly by the formation of bigger aerosols that deposits throughout the tube. Moreover, they were not capable of readily passing through the filters.

3.6. Reducing conditions

The experiments performed under reducing condition, both dry and humid, produced a black thin (it was possible to see the underlying metal surfaces) deposit on the metal surfaces. Considering the color of the deposit, metallic tellurium (Rumble, 2019) is the most likely species. Moreover, for the SEM/EDX a small part of each deposit was removed using an adhesive carbon tape, which after removed indicated no visible effect by the deposit on the underly-

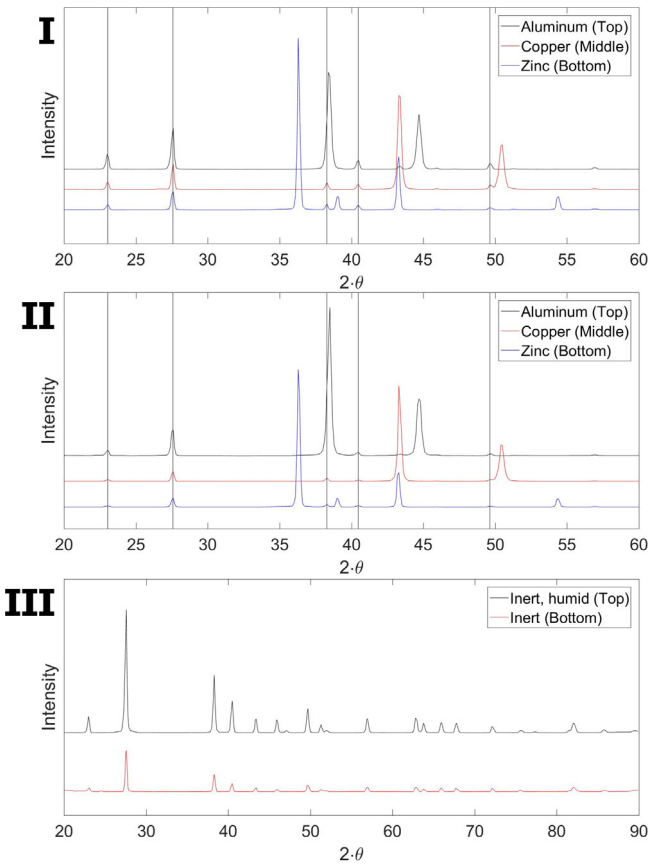

Fig. 5. The X-ray diffraction analyses of the depositions formed on the metal surfaces from dry (**I**) and humid (**II**) inert conditions experiments. Diffractograms for the filter used during these experiments are also shown (**III**).

ing metal surfaces. However, from the visual observation alone, it is not certain that the underlying surfaces were unaffected. A similar black deposit was found on both the filter's surfaces, with a slight white/grey coloration to them. Hence, indicating based on the color metallic tellurium with some possible TeO_2 (Rumble, 2019). Initially, the crucible (porcelain-material) used was severely damaged during the experiment. Essentially, all the parts of the crucible had turned brown-black. However, changing the crucible (to Al_2O_3-material) resolved this and only where the precursor had been added was any coloration noticed.

Moreover, micrographs were produced of the deposits on the aluminum, copper, and zinc surfaces from the reducing condition experiments, both without and with humidity increased. The appearances of these particles are generally as smooth spheres, spike-shaped, and rectangular objects. These micrographs can be seen in Fig. 6. The results from the EDX are presented in Table 6 and indicates that these three types of particles consisted mainly of tellurium, occasionally with the presence of oxygen.

Observing the morphology and elemental composition of the particles. Very little difference exists between the two deposits produced under dry and humid reducing conditions. Moreover, the morphology of the particles observed was similar to those observed in the deposits produced under the inert conditions. Moreover, no other elements were detected by the EDX apart from the carbon and oxygen in the deposits that were removed. Of these elements, the carbon comes from the carbon tape. There are several alternatives for the source of oxygen, ranging from a minor leak during the experiments, contamination during the transportation, and potentially oxygen being released during the formation of H_2Te (Alonso and González, 1991).

The deposits obtained on the different surfaces from the experiments carried out under dry (**I**) and humid (**II**) reducing conditions were analyzed by XRD. In these deposits, diffraction peaks were found in both diffractograms and these were identified as metallic

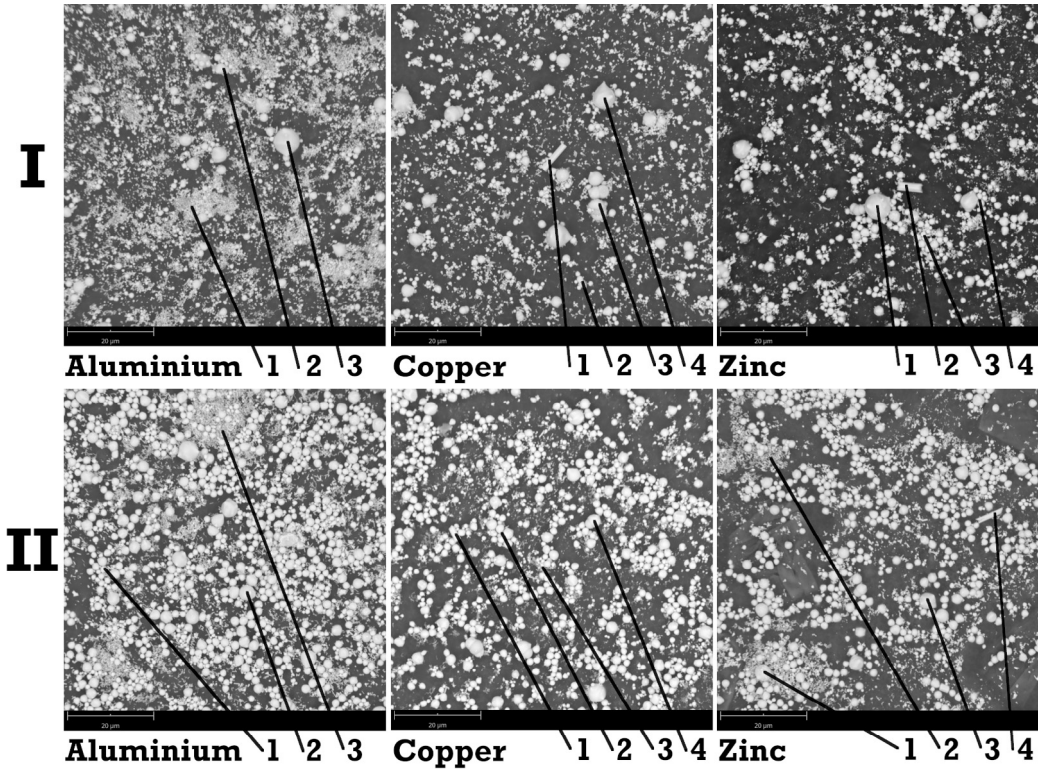

Fig. 6. Six micrographs from dry (**I**) and humid (**II**) reducing conditions experiments, each showing the deposits from the aluminum (left), copper (middle), and zinc (right) surfaces. The locations highlighted have been analyzed and the detected elements are shown in Table 6.

Table 6
The main elements detected using energy dispersive X-ray (EDX) analysis on selected points in the micrographs from both of the reducing conditions, shown in Fig. 6. Except for C, all elements detected are included. Appendix A contains the corresponding EDX spectrum.

	Reducing				Reducing, humid			
Position	1	2	3	4	1	2	3	4
Aluminum	Te	Te	Te		Te	Te	Te	
Copper	Te	Te	Te	Te	Te	Te	Te	Te, O
Zinc	Te	Te	Te	Te	Te	Te	Te	Te

tellurium. These two diffractograms can be seen in Fig. 7. In these diffractograms, the diffraction peaks for metallic tellurium have been highlighted and all other peaks have been determined to come from the underlying bulk materials.

Moreover, the filters located after the coupons under both reducing conditions were also analyzed using XRD. In the deposits formed on these filters, diffraction peaks were found in both diffractograms that were identified as metallic tellurium. The diffractograms (**III**) from these analyses are shown in Fig. 7.

Similarly to the inert conditions, the deposits showed no significant differences under the two reducing conditions or with the deposits formed under inert conditions. Tellurium was detected by XRD analyses in all the deposits from the different surfaces and the filters. However, no other element or species were observed. According to the existing literature (Alonso and González, 1991), tellurium is expected to be the prevailing species at low temperatures. However, at high temperature under humid reducing conditions the species H_2Te would also be expected, which is not stable at lower temperatures (Alonso and González, 1991).

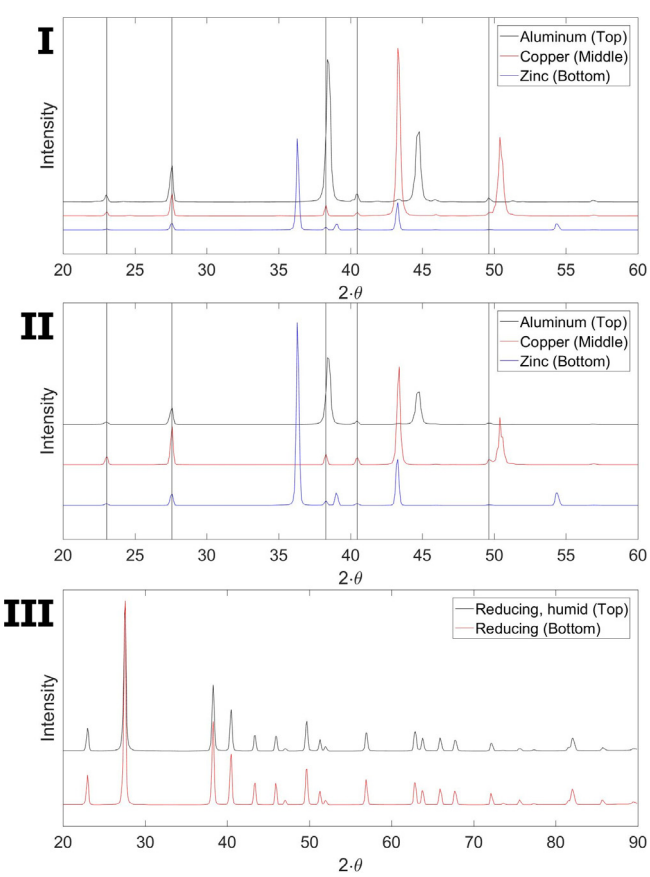

Fig. 7. The X-ray diffracts analyses of the depositions formed on the metal surfaces from the dry (**I**) and humid (**II**) reducing conditions experiments. Diffractograms for the filter used during these experiments are also shown (**III**).

ICP-MS was used to determine the content of tellurium and the content of the metals in the sodium hydroxide liquid traps. Under the humid reducing conditions, significant amounts of both tellurium and noticeable levels of aluminum were observed in the trap, with a mass of $1.1\%_{weight}$ (percent of the original precursor amounts) of tellurium and 0.2 mg of aluminum determined in the original trap volume.

Under the humid reducing conditions, noticeable amounts of aluminum were observed in the corresponding sodium hydroxide liquid trap. For the humid reducing condition the explanation could be that the species H_2Te (Alonso and González, 1991) was interacting with the aluminum surface. However, as the tube itself is made of alumina this could also be a possible source of aluminum. In this case, it is not possible to say with certainty what the source of the aluminum observed in the trap is. Alternatively, as both humid inert and reducing conditions, showed significant levels of aluminum in the traps, it could be that the humidity forms thin films on the tube that enables the airborne tellurium to interact with the aluminum. Consequently, loosening the aluminum so that it is able to be transported to the trap.

4. Conclusions

The main observation between the different investigated conditions (oxidizing, inert, reducing) was the high volatility of tellurium under humid reducing (highest) and humid oxidizing conditions (second highest). Under both these experimental conditions, the tellurium mass reaching the sodium hydroxide liquid traps were comparably high to the other experimental conditions. Moreover, for the transported tellurium to reach the liquid traps it had to pass through a filter. Hence, a potential reason for the observed higher amounts of tellurium could be due to a shift towards smaller sized distribution of the particles transported.

In this work, it was seen that tellurium exposed to high temperatures under different conditions (oxidizing, inert, and reducing), both dry and humid, followed by rapid cooling to room temperature produced noticeable deposition on the surfaces (aluminum, copper, and zinc) investigated herein. No selectiveness for any of the surfaces was observed and no other tellurium species besides TeO_2-orthorhombic (both dry and humid oxidizing), TeO_2-paratellurite (humid oxidizing), and metallic tellurium (inert and reducing) were determined to be present in the different deposits according to the crystal structures. Considering the low temperature at the surfaces location, this would be reasonable.

However, according the IPC-MS analysis of the sodium hydroxide liquid trap from the humid oxidizing condition experiments, both tellurium and zinc were detected. Hence, a potential interaction between them may have occurred. This could be relevant from a source term perspective, as the zinc (e.g, galvanized surfaces or if zinc is used in paint) present in the reactor containment could act either as a sink or could increase the volatility of tellurium. In this

work, the latter is indicated to be true by the observation of both higher amounts of tellurium and zinc in the sodium hydroxide liquid trap. However, the reason why zinc was observed is not clear as the XRD did not detect any species on the zinc surface or the filter (possibly below detection limit). It would seem, however, that the tellurium has a part in this as no zinc was observed in the trap from the corresponding reference case and thus, question remaining is how. A potential explanation could be the formed $TeO(OH)_2$, as it was under condition necessitating the formation of it that the zinc related observation occurred. Alternatively, TeO_2 was dissolved in the water film formed and thereby interacted with the zinc surface.

Additionally, the characterization of the depositions showed that the morphology of the particles under oxidizing conditions was that of round spheres with varied sizes. Under inert and reducing conditions the morphology of the particles was much more varied. In terms of transport to the surface, this characterization provides little information regarding the transportation itself. However, if revolatilization occurs through increases in flow velocity or in other ways this would provide an initial starting state for any parameter (e.g., form factor) requiring such knowledge.

CRediT authorship contribution statement

Fredrik Espegren: Writing - original draft, Conceptualization, Investigation. **Christian Ekberg:** Writing - review & editing, Supervision, Funding acquisition.

Declaration of Competing Interest

The authors declare that they have no known competing financial interests or personal relationships that could have appeared to influence the work reported in this paper.

Acknowledgements

This work was funded by the APRI-10 (Accident Phenomena of Risk Importance), which is supported by the Swedish Radiation Safety Authority (Strålsäkerhetsmyndigheten) and different companies operating different nuclear power plants (i.e., "Forsmarks Kraftgrupp", "OKG", and "Ringhals AB").

Appendix A

See Figs. A.1–A.9.

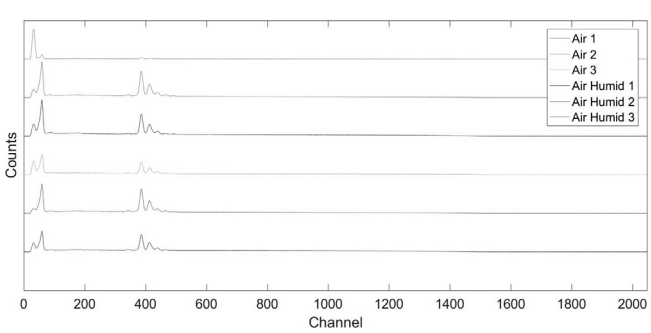

Fig. A.1. The energy dispersive X-ray spectra of the locations in the deposits produced under dry and humid oxidizing conditions from the aluminum surface.

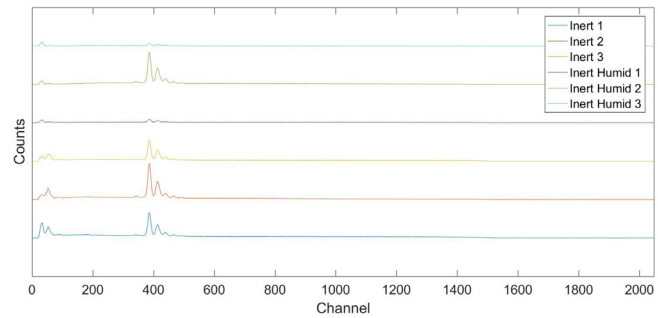

Fig. A.2. The energy dispersive X-ray spectra of the locations in the deposits produced under dry and humid inert conditions from the aluminum surface.

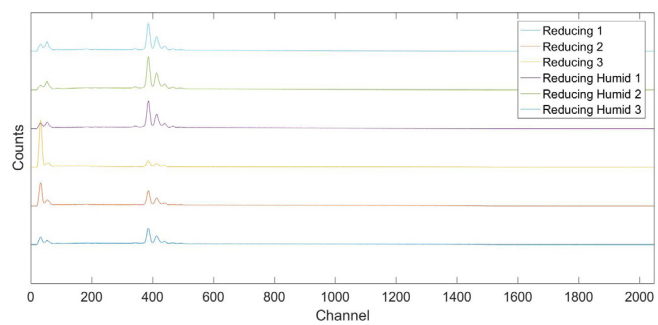

Fig. A.3. The energy dispersive X-ray spectra of the locations in the deposits produced under dry and humid reducing conditions from the aluminum surface.

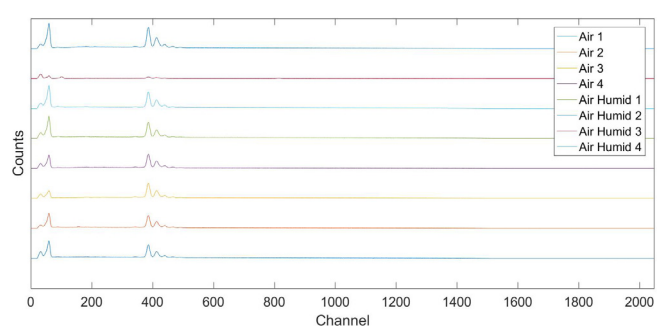

Fig. A.4. The energy dispersive X-ray spectra of the locations in the deposits produced under dry and humid oxidizing conditions from the copper surface.

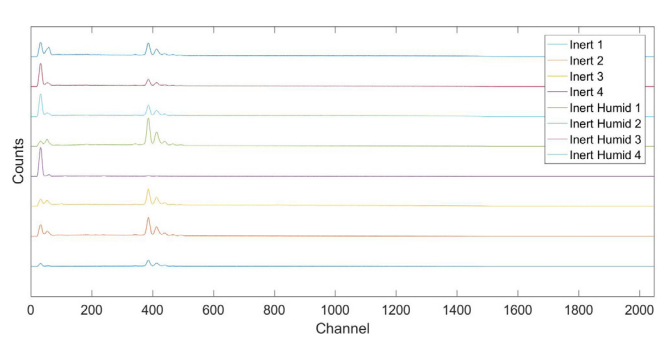

Fig. A.5. The energy dispersive X-ray spectra of the locations in the deposits produced under dry and humid inert conditions from the copper surface.

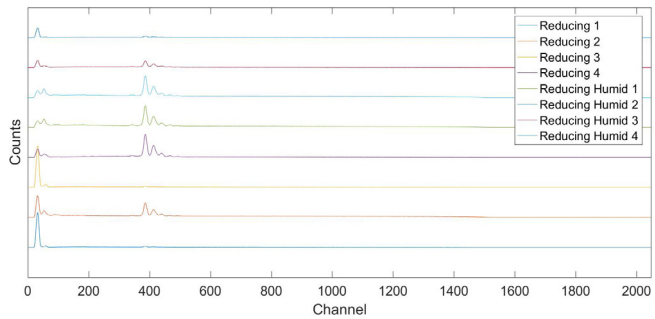

Fig. A.6. The energy dispersive X-ray spectra of the locations in the deposits produced under dry and humid reducing conditions from the copper surface.

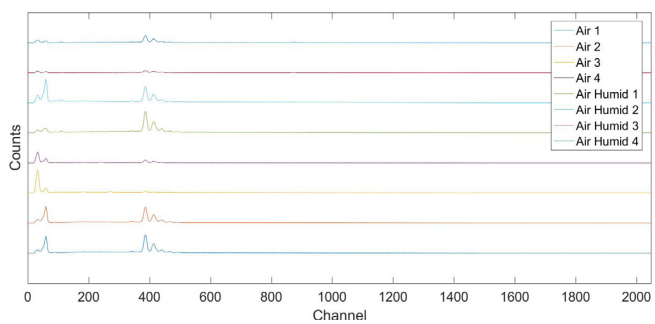

Fig. A.7. The energy dispersive X-ray spectra of the locations in the deposits produced under dry and humid oxidizing conditions from the zinc surface.

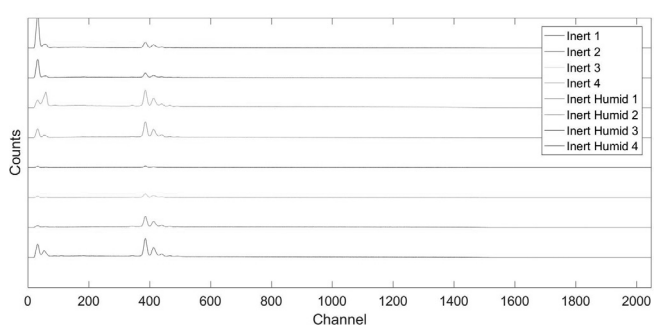

Fig. A.8. The energy dispersive X-ray spectra of the locations in the deposits produced under dry and humid inert conditions from the zinc surface.

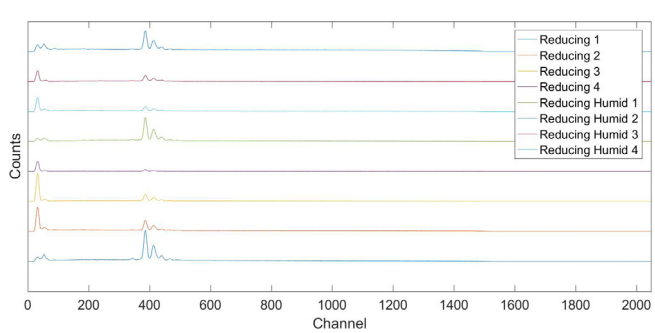

Fig. A.9. The energy dispersive X-ray spectra of the locations in the deposits produced under dry and humid reducing conditions from the zinc surface.

Appendix B. Supplementary data

Supplementary data associated with this article can be found, in the online version, athttps://doi.org/10.1016/j.anucene.2020.107629.

References

Alonso, A., González, C., 1991. Modelling the chemical behaviour of tellurium species in the reactor pressure vessel and the reactor cooling system under severe accident conditions. Report, Commission of the European Communities (CEC), The Joint Research Centre, 1991. EUR–13787..

Beahm, E.C., 1987. Tellurium behavior in containment under light water reactor accident conditions. Nucl. Technol. 78 (3), 295–302.

Bixler, N., Gauntt, R., Jones, J., Leonard, M., 2013. State-of-the-art reactor consequence analyses project volume 1: Peach bottom integrated analysis. Report, Sandia National Laboratories, Albuquerque, New Mexico 87185. NUREG/CR-7110..

Bosland, L., Dickinson, S., Glowa, G.A., Herranz, L.E., Kim, H.C., Powers, D.A., Salay, M., Tietze, S., 2014. Iodine–paint interactions during nuclear reactor severe accidents. Ann. Nucl. Energy 74, 184–199.

Collins, J.L., Osborne, M.F., Lorenz, R.A., 1987. Fission product tellurium release behavior under severe light water reactor accident conditions. Nucl. Technol. 77 (1), 18–31.

de Boer, R., Cordfunke, E.H.P., 1995. Reaction of tellurium with zircaloy-4. J. Nucl. Mater. 223 (2), 103–108.

de Boer, R., Cordfunke, E.H.P., 1997. The chemical form of fission product tellurium during reactor accident conditions. J. Nucl. Mater. 240 (2), 124–130.

Ducros, G., 2012. Fission product release and transport. In: Sehgal, B.R., (Ed.), Nuclear Safety in Light Water Reactors: Severe Accident Phenomenology, chapter 5, first ed., Elsevier. pp. 426–517..

Dutton, W.A., Cooper, W.C., 1966. The oxides and oxyacids of tellurium. Chem. Rev. 66 (6), 657–675.

Glänneskog, H., 2005. Iodine-Metal Surface Interactions under Severe Accident Conditions in a Nuclear Power Plant. (Doctoral thesis at Chalmers University of Technology. No. 2374). Institution of Chemistry and Chemical Engineering, Chalmers University of Technology..

Glänneskog, H., Liljenzin, J.O., Sihver, C., 2006. Reactions between reactive metals and iodine in aqueous solutions. J. Nucl. Mater. 348 (1), 87–93.

Holm, J., Glänneskog, H., Ekberg, C., 2009. Deposition of ruo_4 on various surfaces in a nuclear reactor containment. J. Nucl. Mater. 392 (1), 55–62.

Imoto, S., Tanabei, T., 1988. Chemical state of tellurium in a degraded lwr core. J. Nucl. Mater. 154 (1), 62–66.

Kajan, I., 2016. Transport and Containment Chemistry of Ruthenium under Severe Accident Conditions in a Nuclear Power Plant. (Doctoral thesis at Chalmers University of Technology. No. 4145). Institution of Chemistry and Chemical Engineering, Chalmers University of Technology..

Kajan, I., Lasseson, H., Persson, I., Ekberg, C., 2016. Interaction of ruthenium tetroxide with surfaces of nuclear reactor containment building. J. Nucl. Sci. Technol. 53 (9), 1397–1408.

Magill, J., Pfenning, G., Dreher, R., Sòti, Z., 2015. Karlsruher nuklidkarte, seventh ed..

Malinauskas, A.P., Gooch Jr, J.W., Redman, J.D., 1970. The interaction of tellurium dioxide and water vapor. Nucl. Appl. Technol. 8 (1), 52–57.

McFarlane, J., 1996. Fission product tellurium chemistry from fuel to containment. In: Guentay, S., (Ed.), Proceedings of the Fourth CSNI Workshop on the Chemistry of Iodine in Reactor Safety. (PSI–97-02). Switzerland. pp. 563–585..

Mun, C., Cantrel, L., Madic, C., 2006. Review of literature on ruthenium behavior in nuclear power plant severe accidents. Nucl. Technol. 156 (3), 332–346.

Ning, X., Selesnick, I.W., Laurent, D., 2014. Chromatogram baseline estimation and denoising using sparsity (beads). Chemometrics Intell. Lab. Syst. 139, 156–167.

Pontillon, Y., Ducros, G., Malgouyres, P.P., 2010. Behaviour of fission products under severe pwr accident conditions vercors experimental programme—part 1: general description of the programme. Nucl. Eng. Design 240 (7), 1843–1852.

Rumble, J.R., 2019. Fission product release and transport. In J.R. Rumble, editor, In CRC Handbook of Chemistry and Physics, chapter 5. CRC Press/Taylor & Francis, Boca Raton, FL, 100 (internet version 2019 edition)..

Tietze, S., 2015. The chemistry of organic iodides under severe nuclear accident condtions in LWRs. (Doctoral thesis at Chalmers University of Technology. No. 3839). Institution of Chemistry and Chemical Engineering, Chalmers University of Technology..

van Brussel, B.A., De Hosson, J.Th.M., 1994. Glancing angle x-ray diffraction: a different approach. Appl. Phys. Lett. 64 (12), 1585–1587.

Yoshida, S., Ojino, M., Ozaki, T., Hatanaka, T., Nomura, K., Ishii, M., Koriyama, K., Akashi, M., 2014. Guidelines for iodine prophylaxis as a protective measure: Information for physicians. Jpn. Med. Assoc. J. 57 (3), 113–123.